Journal of Thermal Analysis, Vol. 35 (1989) 1441–1458

KINETIC ANALYSIS OF CONSECUTIVE REACTIONS USING TG AND DSC TECHNIQUES

Theory and Application

D. Skala, M. Sokić, J. Tomić and *H. Kopsch*[+]

FACULTY OF TECHNOLOGY AND METALLURGY, 11001 BELGRADE,
P.O. BOX 494, KARNEGIJEVA 4, YUGOSLAVIA
[+]GERMAN INSTITUTE FOR PETROLEUM RESEARCH,
3392 CLAUSTHAL-ZELLERFELD, W. NERNST STR. 7, F. R. GERMANY

(Received May 11, 1988)

A complex mechanism of thermal degradation processes was postulated for the reaction type $A \xrightarrow{k_1} R \xrightarrow{k_2} S$, and a theoretical analysis of DTG and DSC curves was followed by corresponding mathematical simulation. In this scheme, compound S represents a volatile product (e.g. gas and/or vapor), which is a necessary assumption in order to explain the differences in results which can arise after the kinetic analysis of DTG and DSC experimental data.

Mathematical simulation was performed with different values of the Arrhenius parameter for both reaction rate constants (k_1 and k_2) in the range 83.1–291.0 kJ/mol for the activation energy and with corresponding values for the frequency factor (10^5–10^{19} min^{-1}). The influence of endothermic heat effects (50–200 kJ/mol) in the reactions $A \rightarrow E$ and $R \rightarrow S$ was also investigated. The calculated rates of mass and heat change (DTG and DSC), for different heating rates, showed that the maximum values of the two curves are reached at different temperatures. The non-uniformity of the DTG and DSC maxima depends on the difference between the values of the reaction rate constants and their temperature sensitivities (E_1 and E_2), and also on the heating rate.

The theoretical analysis performed demonstrated the possibility of determining the reaction rate parameters (k_1 and k_2) in the case of consecutive first-order reactions, by using simultaneous TG and DSC analysis.

The proposed theoretical analysis is supported by experimental DTG/DSC data concerning the pyrolysis of oil shale, which were interpreted in terms of consecutive reactions.

TG and DSC analysis have been extensively used to study the kinetics of different reactions in the solid state, as well as the kinetics of thermal degradation of different polymeric materials, bitumen, wood, heavy oil, coal, and oil shale. Although many results have been derived by assuming that a simple and single reaction is involved

John Wiley & Sons, Limited, Chichester
Akadémiai Kiadó, Budapest

in the thermal decomposition (e.g. a first-order reaction), they gave valuable information about the temperature-dependence of the thermal degradation processes. Actually, all the above-mentioned processes are very complex in nature and involve a set of many simultaneous parallel and consecutive reactions. The need was therefore recognized for suitable methodology to analyse the experimental data obtained with sophisticated techniques. Some recent attempts were concerned with the goal of interpreting the complex reaction via parallel TG and DSC results [1–4]. Agrawal [2] has discussed some results of DSC and TG analysis, especially for the situation where different kinetic parameters can be obtained, stipulating that if a reaction occurs with both a change in weight and a change in the heat of reaction, the kinetic parameters derived from TG and DSC under the same experimental conditions should be identical. On the other hand, some of our recently published results [5] on the kinetics of Aleksinac oil shale pyrolysis have shown large differences in the Arrhenius parameters obtained from TG and DSC data. This could be explained by the existence of a complex mechanism of oil shale pyrolysis, and by the different methods used to interpret TG (the integral method of Doyle–Gorbachev [6] with a first-order reaction) and DSC data (the ASTM E 698 standard procedure [7], based on the Kissinger analysis [8]). The second explanation was tested by using the same method to interpret the TG and DSC data, i.e. by analysing the relation between the maximum temperatures of the DTG and DSC curves, and the heating rates [7, 9]. In all cases, when a large disproportionality was observed between the mass change and the heat effect, a pronounced difference was registered in the DTG and DSC derived Arrhenius parameters.

In this paper, consecutive reactions are used to demonstrate the possibility of interpreting simultaneous DTG and DSC data. The basis is the two-step decomposition process of oil shale pyrolysis

$$\text{kerogen} \rightarrow \text{bitumen} \rightarrow \text{oil} + \text{gas}$$

first postulated by Engler [10] and extensively used in subsequent interpretations of the kinetics of oil shale pyrolysis [11–13].

Theoretical analysis of DTG and DSC maxima

DTG and DSC derived kinetic parameters for the thermal decomposition of organic materials such as kerogen can be determined by using the maximum rate method [7, 8, 14]. The procedure is based on the application of Eq. (1):

$$\frac{E}{RT_m^2} = \frac{A}{q} \exp\left(-\frac{E}{RT_m^2}\right) \tag{1}$$

When the logarithmic values of the heating rate were plotted versus the reciprocal temperatures of the DTG and DSC maxima, the activation energy and frequency factor could be determined from the slope and intercept of the resulting straight line.

For a simple reaction defined by the stoichiometric equation:

$$A \xrightarrow{k} f_1 R + f_2 S \tag{2}$$

simultaneously performed DTG and DSC analysis gave identical results when Eq. (1) was applied. However, different results can be obtained in the case of a complex reaction such as the thermal degradation of kerogen [11, 12, 15]. The general outline of the complex degradation process is presented in Fig. 1.

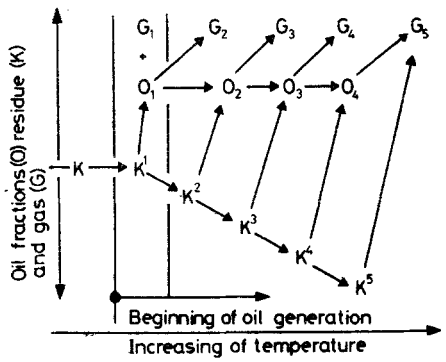

Fig. 1 Schematic presentation of oil and gas formation during the pyrolysis of kerogen

If only the first two reaction steps are taken into account [13], the mechanism of the complex process is defined by Eqs (3a) and (3b). The mathematical simulation of the DTG and DSC curves can be performed by using a simplification postulated in advance by Eq. (3c):

$$K \xrightarrow{k_1} f_1 K_1 + f_2 G_1 \tag{3a}$$

$$K_1 \xrightarrow{k_2} f_3 K_2 + f_4 G_2 \tag{3b}$$

$$f_2 \ll f_1; \quad f_3 \ll f_4 \tag{3c}$$

This is an acceptable assumption in the case of a complex reaction in which a large heat absorption effect predominates in the first step, without any or with only a very small mass change, and the corresponding heat absorption effect in the next

step is accompanied by mass change [13]:

$$A_{(\text{solid})} \xrightarrow[Q_1]{k_1} R_{(\text{solid}^*)} \xrightarrow[Q_2]{k_2} S_{(\text{volatile compounds})} \tag{4}$$

Mathematical simulation had the purpose of showing the characteristic peaks of DTG and DSC curves, i.e. the temperatures at which the maximum rates of mass change (DTG-max) and heat absorption (DSC-max) occur.

The simulation of DTG and DSC curves was based on the statement that the rates of both reactions in Eq. (4) are defined by a first-order relationship, as in Eqs (5)–(7):

$$(-r_A) = -\frac{\mathrm{d}m_A}{\mathrm{d}T} = \left(\frac{A_1}{q}\right) \cdot m_A \cdot \exp\left(-\frac{E_1}{RT}\right) \tag{5}$$

$$(r_R) = \frac{\mathrm{d}m_R}{\mathrm{d}T} = \left(\frac{A_1}{q}\right) m_A \exp\left(-\frac{E_1}{RT}\right) - \left(\frac{A_2}{q}\right) m_R \exp\left(-\frac{E_2}{RT}\right) \tag{6}$$

$$(r_S) = \frac{\mathrm{d}m_S}{\mathrm{d}T} = \left(\frac{A_2}{q}\right) \cdot m_R \cdot \exp\left(-\frac{E_2}{RT}\right) \tag{7}$$

Volatile compounds (gas and vapor) are produced only in the second stage; this means that the rate of S-formation can be detected by DTG analysis, via Eq. (8), while the rates of A-consumption and S-formation determine the overall heat absorption rate which can be detected by DSC analysis, via Eq. (9):

$$\mathrm{DTG} = r_S = \left(\frac{A_2}{q}\right) \cdot m_R \cdot \exp\left(-\frac{E_2}{RT}\right) \tag{8}$$

$$\begin{aligned} \mathrm{DSC} &= Q_1 \cdot (-r_A) + Q_2 \cdot (r_S) = \\ &= \frac{Q_1 A_1}{q} \cdot m_A \cdot \exp\left(-\frac{E_1}{RT}\right) + \frac{Q_2 A_2}{q} \cdot m_R \cdot \exp\left(-\frac{E_2}{RT}\right) \end{aligned} \tag{9}$$

Differentiation of Eqs (8) and (9) with respect to T gives the differential form, from which it is easy to solve the necessary conditions which must be satisfied for the existence of DTG and DSC maxima: $(\partial[\mathrm{DTG}]/\partial T) = 0$ and $(\partial[\mathrm{DSC}]/\partial T) = 0$. If T_1 represents the temperature of the DTG maximum and T_2 the corresponding temperature of the DSC maximum, the necessary conditions for the existence of maxima are defined by Eqs (10) and (11):

$$\left[\frac{m_R}{m_A}\right]_{\text{at } T_1} = \left\{\frac{k_1}{k_2 - (q \cdot E_2)/T^2}\right\}_{\text{at } T_1} \tag{10}$$

$$\left[\frac{m_R}{m_A}\right]_{\text{at } T_2} = \left\{\frac{k_1 \cdot E_1 \cdot \bar{Q} + (k_1 \cdot k_2/q) \cdot T^2 - (k_1^2/q) \cdot \bar{Q} \cdot T^2}{k_2[(k_2 \cdot T^2/q) - E_2]}\right\}_{\text{at } T_2} \tag{11}$$

where $\bar{Q}$ denotes the ratio of the heat effects Q_1 and Q_2, both with a negative sign as a consequence of the assumption that $A \rightarrow R$ and $R \rightarrow S$ are endothermic reactions.

It is obvious that Eqs (10) and (11) indicate different positions of the maxima of the DTG and DSC curves. However, the question arises as to whether it is possible to obtain both maximum values at the same temperature for different heating rates, i.e. $T_1 = T_2$. In this case, only one value of A and E would be obtained from Eq. (1).

Assuming that $T = T_1 = T_2$, and also that $k = k_1 = k_2 = A \cdot \exp(-E/RT)$, Eqs (10) and (11) give the relation defined by Eq. (12), which indicates that this is not possible (T_1 must differ from T_2) unless some other specific conditions are valid:

$$\left[\frac{m_R}{m_A}\right]_{\text{DSC}} = -\bar{Q} + \left[\frac{m_R}{m_A}\right]_{\text{DTG}} \tag{12}$$

Analysis of conditions where $T_1 = T_2$ *(*$DTG_{max} = DSC_{max}$*)*

Equations (10) and (11) can be expressed in a form suitable for further discussion:

$$\left[\frac{m_R}{m_A}\right]_{\text{at } T_1} = \frac{k_1(T_1)}{\Delta k_2(T_1)} \tag{10a}$$

$$\left[\frac{m_R}{m_A}\right]_{\text{at } T_2} = \frac{k_1(T_2)}{\Delta k_2(T_2)}\left[1 - \bar{Q}\frac{\Delta k_1(T_2)}{k_2(T_2)}\right] \tag{11a}$$

where Δk_1 and Δk_2 are defined by Eqs (13) and (14):

$$\Delta k_1 = k_1 - (q \cdot E_1/T^2) \qquad \text{at } T = T_1 \tag{13}$$

$$\Delta k_2 = k_2 - (q \cdot E_2/T^2) \qquad \text{at } T = T_1 \text{ or } T = T_2 \tag{14}$$

Equation (10a) has meaning only if $\Delta k_2(T_1) > 0$. The equality between the conditions for DSC-max and DTG-max, i.e. the relation $T = T_1 = T_2$, is fulfilled if $\Delta k_1(T_2) = 0$ or $\bar{Q} = 0$. The first condition is expressed by Eq. (15), i.e. by Eq. (1):

$$q\frac{E_1}{T_2^2} = A_1 \cdot \exp\left(-\frac{E_1}{RT_2}\right) \tag{15}$$

which shows that in the case of equal temperatures T_1 and T_2 registered by TG and DSC analysis at different heating rates, only E_1 and A_1 can be determined. The second condition ($\bar{Q} = 0$) is not of interest because the present analysis is concerned with a consecutive reaction in which a larger heat effect is associated with the first reaction step.

Moreover, the condition $\Delta k_1(T_2) = 0$ indicates that simultaneous TG/DSC is practically useless for the investigation of rate constants of consecutive reactions. Nevertheless, a more important conclusion can be obtained in the case when Δk_1 and Δk_2, defined by Eqs (13) and (14), are greater than zero and $\bar{Q} > 0$. Then, Eqs (10a) and (11a) give:

$$\left[\frac{m_R}{m_A}\right]_{T_2} < \left[\frac{m_R}{m_A}\right]_{T_1} \tag{16}$$

Equation (16) shows that the sequence of appearance of DTG-max and DSC-max depends on the ratio of the rates of the consecutive reaction steps.

Mathematical simulation of m_R/m_A; change with temperature

Mathematical simulation of the reaction given by Eq. (4) was performed in order to identify the positions of the maximum mass change rate and the heat absorption rate for different combinations of the rate constants k_1 and k_2. This information was then used to determine the kinetic parameters via Eq. (1). Comparison of the determined kinetic parameters with those used in the simulation was assumed to be a proper indication of the possibilities that simultaneous DTG and DSC analysis offer in the kinetic investigations of consecutive reactions.

The simulation consists in solving Eqs (5)–(11) in the temperature range 573–973 K, which is of practical importance in oil shale pyrolysis. Equations (5)–(7) were solved by using the Runge–Kutta method of the fourth order, with the initial conditions: $T_0 = 573$ K; $m_{A0} = 1$; $m_{R0} = m_{S0} = 0$. The temperature increment was 0.5 deg up to a value of 973 K. The calculated values of m_A, m_R and m_S were used in Eqs (8)–(11), together with the corresponding temperatures. The positions of the maxima in the DTG and DSC curves are indicated by the cross-section of the curve $m_R/m_A = f_1(T)$ and the curves which correspond to Eqs (10) and (11), respectively. The calculational procedure was repeated with heating rate values of 2, 5, 10 and 20 deg/min.

Different combinations of the rate constants, denoted as cases I, II and III, were used in the simulations:

Case I

$$k_1 = 10^{13} \exp(-25{,}000/T),\ \text{min}^{-1}$$
$$k_2 = 10^{5} \exp(-10{,}000/T),\ \text{min}^{-1}$$

Case II

$$k_1 = 10^{13} \exp(-29{,}000/T),\ \text{min}^{-1}$$
$$k_2 = 10^{5} \exp(-10{,}000/T),\ \text{min}^{-1}$$

Case III

$$k_1 = 10^7 \exp(-15{,}000/T), \text{ min}^{-1}$$
$$k_2 = 10^{19} \exp(-35{,}000/T), \text{ min}^{-1}$$

The kinetic parameters used in case I are similar to those reported for Aleksinac oil shale pyrolysis [5]. The other two combinations were selected in order to simulate different situations with regard to the relative rates of the consecutive reaction steps. The dependences of k_1/k_2 on temperature for cases I–III are shown in Fig. 2.

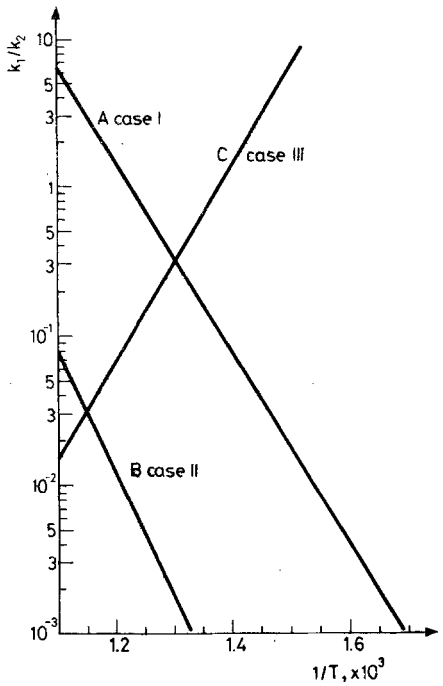

Fig. 2 Arrhenius plot for the ratio k_1/k_2

Results and discussion

The calculated values of T_{max} for DTG (T_1) and DSC (T_2) for cases I–III are presented in Table 1, together with the determined kinetic parameters from Eq. (1) and data on the ln (q) versus $1/T_1$ or $1/T_2$ dependence.

General remarks concerning the presented results can be presented briefly as:

Case I: The reactivity of intermediate R is very low. The condition defined by Eq. (16) is fulfilled for all the investigated heating rates. The change of m_R/m_A with

Table 1 Results of mathematical simulation

Case	q, deg/min	T_1, K	T_2, K	$\bar{Q}$	Kinetic parameters Eq. (1)			
					DTG-max		DSC-max	
					E, K (corr. coeff. r)	A, min^{-1}	E, K (corr. coeff. r)	A, min^{-1}
	2	778.5	773.0	4				
	5	805.5	795.0	4	21640	$7.38 \cdot 10^{10}$	26250	$4.42 \cdot 10^{13}$
	10	826.3	811.5	4	($r = 0.999$)		($r = 0.999$)	
	20	849.0	829.3	4				
	2	778.5	775.5	1				
I	5	805.5	798.5	1	21640	$7.38 \cdot 10^{10}$	24792	$5.62 \cdot 10^{13}$
	10	826.3	817.2	1	($r = 0.999$)		($r = 0.999$)	
	20	849.0	835.5	1				
	2	778.5	777.5	0.25				
	5	805.5	802.0	0.25	21640	$7.38 \cdot 10^{10}$	22630	$2.95 \cdot 10^{11}$
	10	826.3	823.0	0.25	($r = 0.999$)		($r = 0.999$)	
	20	849.0	844.0	0.25				
	2	893.0	892.0	4				
	5	917.0	916.0	4	29220	$1.10 \cdot 10^{13}$	30690	$6.40 \cdot 10^{13}$
	10	936.0	935.5	4	($r = 0.998$)		($r = 0.999$)	
	20	961.0	956.0	4				
	2	893.0	893.0	1				
II	5	917.0	914.2	1	29220	$1.10 \cdot 10^{13}$	27950	$3.12 \cdot 10^{12}$
	10	936.0	935.5	1	($r = 0.998$)		($r = 0.999$)	
	20	961.0	957.0	1				
	2	893.0	893.0	0.25				
	5	917.0	914.0	0.25	29220	$1.10 \cdot 10^{13}$	27710	$2.39 \cdot 10^{12}$
	10	936.0	936.0	0.25	($r = 0.998$)		($r = 0.999$)	
	20	961.0	957.5	0.25				
	2	780.9	781.2	4				
	5	800.5	816.4	4	15190	$1.44 \cdot 10^{7}$	17920	$3.62 \cdot 10^{8}$
	10	842.8	849.0	4	($r = 0.982$)		($r = 0.993$)	
	20	878.1	880.1	4				
	2	780.9	781.3	1				
III	5	800.5	802.4	1	15190	$1.44 \cdot 10^{7}$	15040	$1.14 \cdot 10^{7}$
	10	842.8	847.2	1	($r = 0.982$)		($r = 0.984$)	
	20	878.1	879.6	1				
	2	780.9	781.3	0.25				
	5	800.5	801.0	0.25	15190	$1.44 \cdot 10^{7}$	14180	$3.72 \cdot 10^{6}$
	10	842.8	844.6	0.25	($r = 0.982$)		($r = 0.980$)	
	20	878.1	879.0	0.25				

temperature is presented schematically in Fig. 3, together with the corresponding solutions of Eqs (10) and (11). As a consequence of the monotonically increasing function m_R/m_A and the conditions defined by Eq. (16), DSC-max appears at lower temperatures than DTG-max (Table 1). When these data were used as the basis for calculation of E and A for an irreversible first-order reaction, $A \xrightarrow{k}$ product, different Arrhenius parameters were determined. With temperature T_2, at which

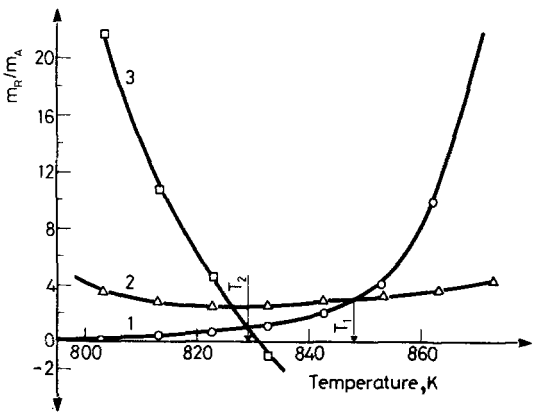

Fig. 3 The simulation curves: 1 – (m_R/m_A) defined by solving the system Eqs (5)–(7); 2 – condition for DTG-max (Eq. (10)); 3 – condition for DSC-max (Eq. (11)). Case I, q = 20 deg/min

DSC-max appears, values of A and E very similar to the corresponding values for k_1 were obtained, while the same analysis based on T_1 and DTG-max data gave A and E which are some combination of the assumed values of A and E for k_1 and k_2.

Case II: The function k_1/k_2 also has a monotonically increasing tendency. This has the same consequences on the change of m_R/m_A with increasing temperature. DTG-max and DSC-max are very close to one another, fulfilling the condition defined by Eq. (16), i.e. the same sequence in the appearance of the maximum in the heat absorption rate and the rate of mass change as obtained in case $I(T_2 < T_1)$. The analysis of T_1 and T_2 in relation to Eq. (1) gives practically the same values of the Arrhenius parameters corresponding to the values of k_1. The above results are in agreement with theoretical analysis and the conclusions expressed in the simple form by Eq. (16) (Fig. 4).

Case III: k_2 is more strongly influenced by temperature than is k_1 $(E_2 > E_1)$, which results in a drastic decrease in k_1/k_2, but also a decrease in m_R/m_A with increasing temperature. The degradation process of intermediate R is faster than the thermal decomposition of reactant A. With the condition defined by Eq. (16) fulfilled, DTG-max appears at a lower temperature than DSC-max (Fig. 5). The

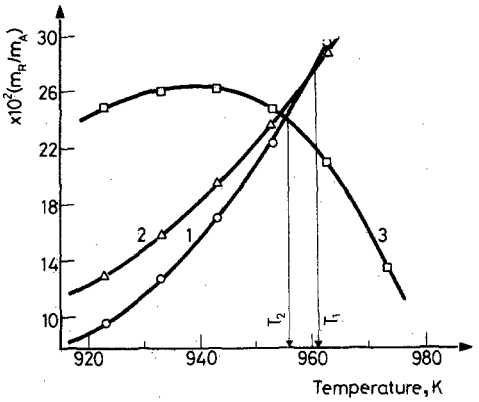

Fig. 4 The simulation curves (same notations as in Fig. 3). Case II, q = 20 deg/min

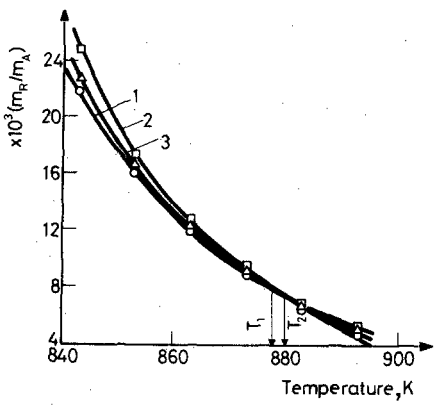

Fig. 5 The simulation curves (same notations as in Fig. 3). Case III, q = 20 deg/min

two temperatures T_1 and T_2 are very close (Table 1), resulting in practically the same E and A calculated via Eq. (1).

Influence of $\bar{Q} = Q_1/Q_2$: In the presented calculation, two different values for Q_1 and Q_2 (50 and 200 kJ/mol) were combined, which corresponds to a $\bar{Q}$ parameter equal to 4, 1, and 0.25. Greater differences between T_1 and T_2, in all calculations, were obtained for a larger heat absorption effect in the first stage ($\bar{Q}$ = 4). These results confirmed theoretical analysis about the influence of $\bar{Q}$ on the T_1 and T_2 differences, as in Eqs (10) and (11).

Analysis of conditions corresponding to greater differences between temperatures at which DTG-max and DSC-max appear

Small differences between the r.h.s. of Eqs (10) and (11) were determined by using data from Table 1 in cases II and III. Equation (15) can be used to predict the difference between T_1 and T_2. Simulated TG data have shown that DSC analysis, as a basis for making the ln (q) versus $1/T_2$ plot, in all cases gives values of A and E very close to the Arrhenius parameter for k_1. On the other hand, the same relationship, when used for the correlation of DTG data, gave values for A and E which differ more or less from the A_2 and E_2 values, depending on the extent to which Eq. (15) is fulfilled.

Obviously, the information about T_2 and $\Delta k_1(T_2)$ can serve as a parameter for predicting the importance of DTG-max data. Such an analysis of the relative differences $\Delta k_1(T_2)/k_1(T_2)$ is shown in Table 2 for cases I–III.

Table 2 Analysis of the difference between T_1 and T_2 which can be expected from DSC data (T_2 values are from Table 1, $\bar{Q} = 4$)

Case	q, deg/min	T_2, K	$k_1(T_2)$, min^{-1}	$q \cdot E_1/T_2^2$, min^{-1}	$\Delta k_1(T_2)/k_1(T_2)$, %
I	2	773.0	0.090	0.084	6.0
	5	795.0	0.220	0.198	10.0
	10	811.5	0.417	0.380	8.9
	20	829.3	0.809	0.727	10.1
II	2	892.0	0.076	0.073	3.9
	5	916.0	0.178	0.173	2.8
	10	935.5	0.344	0.331	5.4
	20	956.0	0.669	0.635	8.4
III	2	781.2	0.046	0.049	6.5
	5	816.4	0.105	0.112	6.7
	10	849.0	0.212	0.208	1.9
	20	880.1	0.395	0.387	2.2

The presented results indicate that only in cases I and II can larger differences between T_1 and T_2 be expected. In such cases, simulation of the thermal degradation process via a complex reaction will give better results than those obtained on the basis of a simple first-order reaction. Simultaneously performed DTG and DSC analysis can be used for k_1 and k_2 determination; k_1 from DSC data, and k_2 partially from DTG data, but only as initial information on the k_2 *vs.* temperature dependence.

Application of theoretical results on oil shale pyrolysis

The presented theory was tested by using the results of oil shale pyrolysis. Non-isothermal pyrolysis was performed with oil shale samples denoted Es and Kor, originating from Estonia, USSR and North Korea, using Stanton–Redcroft TG/DTG/DSC 780 Series instruments. The experimental conditions were similar to those described previously [5]. The temperatures at which DTG and DSC maxima were detected for Es and Kor are given in Table 3.

Table 3 Temperatures of DTG-max (T_1) and DTG-max (T_2) determined in the pyrolysis of oil shale

q, deg/min	Es		Kor	
	T_1, K	T_2, K	T_1, K	T_2, K
5	708.0	707.0	722.0	727.0
10	722.0	717.0	738.0	743.0
20	740.0	729.0	756.0	763.0

The T_1 and T_2 values and the ASTM E–698 procedure [7] were used to calculate the kinetic parameters for the Es and Kor samples, assuming a first-order reaction:

Es oil shale

$$\text{DSC data:} \quad k_{DSC} = 3 \cdot 10^{19} \exp(-33{,}260/T), \text{ min}^{-1}$$
$$\text{DTG data:} \quad k_{DTG} = 8.7 \cdot 10^{12} \exp(-23{,}300/T), \text{ min}^{-1}$$

Kor oil shale

$$\text{DSC data:} \quad k_{DSC} = 1.5 \cdot 10^{12} \exp(-21{,}000/T), \text{ min}^{-1}$$
$$\text{DTG data:} \quad k_{DTG} = 3.5 \cdot 10^{12} \exp(-22{,}000/T), \text{ min}^{-1}$$

The data presented in Table 3 indicate the opposite sequence of appearance of T_1 and T_2 for Es and Kor. On the assumption that oil shale pyrolysis can be properly simulated as a consecutive reaction, as considered in this paper, the following calculation was done.

Es — Estonian oil shale

As a consequence of the sequence of appearance of T_1 and T_2, E_1 values higher than E_2 can be used in the simulation, with a similar effect to that taken into account in Case I. The DSC and DTG data indicate that $E_1 > E_2$ (33,260 compared to 23,300), but still not enough so to give the correct conversion of kerogen when such values are used for pyrolysis simulation (Fig. 6).

Four simulation curves are shown in Fig. 6; *A* and *B* correspond to the assumption that the kerogen degradation of oil shale is a single first-order reaction with rate constants equal to k_{DSC} and k_{DTG} (curves *A* and *B*, respectively). The simulation curve *C* was calculated by assuming that the consecutive reaction $A \xrightarrow{k_{DSC}} R \xrightarrow{k_{DTG}} S$ exists. Obviously, the best fit with the experiment was achieved with curve *D*. This was obtained with a small modification of the rate

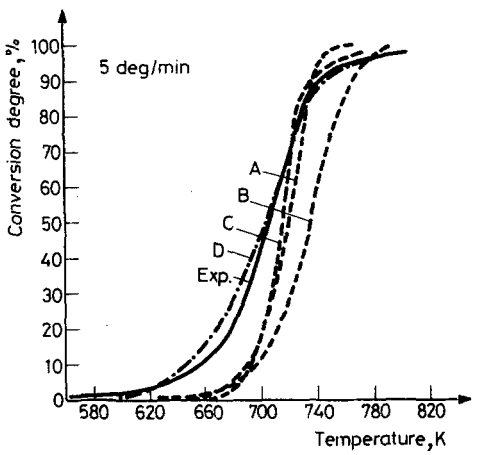

Fig. 6 TG curve of Estonian oil shale: exp – experimental data; *A* and *B* – single first-order reaction with reaction rate constants k_{DSC} and k_{DTG}, respectively; *C* – two-step consecutive model (Eq. (4)); *D* – consecutive reaction model (Eqs (3a) and (3b)) with optimum stoichiometric coefficient $f_1 \div f_4$

constants k_{DSC} and k_{DTG} in the sense of the previously derived conclusion about the usage of simultaneous DTG/DSC data for the analysis of complex reactions. Further, the stoichiometric coefficient (f_1, f_2, f_3 and f_4) in Eqs (3a) and (3b) were modified according to the effect registered by simulation curve *A*. In all the curves (*A*, *B* and *C*), a certain delay in conversion could be observed at lower temperatures, which was followed by a large influence of temperature on the kerogen conversion rate (dX/dT) at temperatures greater than the maximum in the rate of mass loss or heat absorption (DTG-max or DSC-max). The best fit of curve *D* in Fig. 6 was obtained with the following stoichiometric scheme:

$$K \xrightarrow{\hat{k}_{DSC}} 0.92\, K_1 + 0.08\, G_1 \quad \hat{k}_{DSC} = 5.0 \cdot 10^{19} \exp(-29{,}500/T),\ \text{min}^{-1}$$

$$K_1 \xrightarrow{\hat{k}_{DTG}} 0.05\, K_2 + 0.95\, G_2\, k_{DTG} \quad = 9.6 \cdot 10^{8} \exp(-16{,}000/T),\ \text{min}^{-1}$$

Kor — North Korean oil shale

The heat absorption maximum (DSC-max) appears at higher temperatures than the maximum in the rate of mass loss (Table 3). According to the results of the theoretical analysis presented in this paper, such an effect corresponds to Case III. Appropriate simulation curves, as those shown in Fig. 6, together with the experimental data, are presented in Fig. 7. Curves *A* and *B* were calculated by using

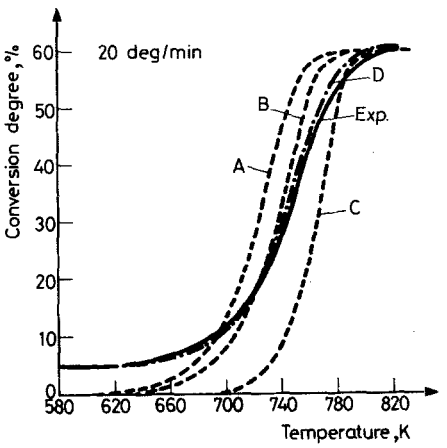

Fig. 7 TG curve of North Korean oil shale: exp – experimental data; *A* and *B* – single first-order reaction with reaction rate constants k_{DSC} and k_{DTG}, respectively; *C* – consecutive reaction (Eq. (4)); *D* – consecutive reaction defined by Eqs (3a) and (3b) with optimum stoichiometric coefficient $f_1 \div f_4$

k_{DSC} and k_{DTG} in the single first-order reaction model, and curve *C* by using the consecutive reaction model $A \xrightarrow{k_{DSC}} R \xrightarrow{k_{DTG}} S\uparrow$. In cases *A* and *B* the influence of temperature on kerogen conversion is more marked, while *C* shows a certain delay at lower temperatures, and a rapid increase in conversion at the end of pyrolysis. The temperature-dependence of k_{DSC} and k_{DTG} was not corrected, and only correction of the stoichiometric coefficient of the consecutive reactions, Eqs (3a) and (3b), was necessary to achieve the best fit of curve *D* (Fig. 7). Curve *D* was obtained by using the following stoichiometric scheme:

$$K \xrightarrow{k_{DSC}} 0.58\,K_1 + 0.42\,G_1 \quad k_{DSC} = 1.5 \cdot 10^{12} \exp(-21{,}000/T),\ \mathrm{min}^{-1}$$

$$K_1 \xrightarrow{k_{DTG}} 0.27\,K_2 + 0.73\,G_2 \quad k_{DTG} = 3.5 \cdot 10^{12} \exp(-22{,}000/T),\ \mathrm{min}^{-1}$$

The influence of heating rate on the quality of simulation is shown in Fig. 8.

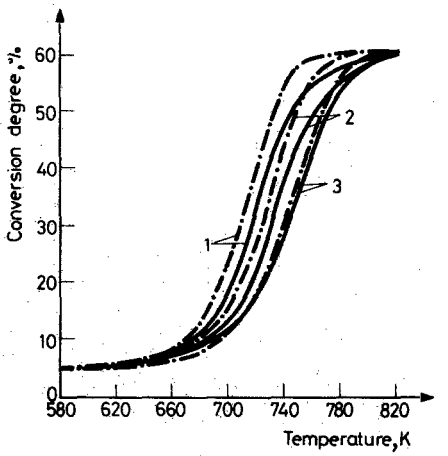

Fig. 8 Comparison of TG experimental data and simulated curve based on consecutive reaction model (——— experimental curve, – – – simulation); 1 – 5 deg/min; 2 – 10 deg/min; 3 – 20 deg/min

Conclusions

Simultaneous TG and DSC analysis offers the possibility of determining the kinetic parameters of the complex thermal degradation process which can be presented by a consecutive reaction of first-order $A \xrightarrow{k_1} R \xrightarrow{k_2} S$ (e.g. thermal degradation of kerogen from oil shale).

The mathematical simulation of the DTG/DSC data was performed in a range of temperatures of practical interest in oil shale pyrolysis, and the results obtained showed that Eq. (16) is fulfilled.

The increase or decrease in the ratio k_1/k_2 with temperature depends on the absolute values of E_1 and E_2. For $E_1 > E_2$, the temperature at which DSC-max is observed (T_2) is lower than T_1 (DTG-max). The reverse sequence of appearance in DSC-max and DTG-max ($T_2 > T_1$) is obtained in the case $E_2 < E_1$.

It should be pointed out that, if the data from simultaneous DTG/DSC analysis are used together with the assumption of existing consecutive reactions, the following kinetic parameters may be calculated:

a) The rate constant k_1 from the DSC data (fairly well).

b) The ratio between the activation energies of the first and second steps of the consecutive reaction, from the DTG and DSC data, i.e. the temperature-dependence for k_2. For exact determination of the Arrhenius equation for k_2, a trial-and-error procedure must be applied, with experimental DTG/DSC data.

The theoretical analysis presented in this paper was used in the kinetic

investigation of oil shale pyrolysis. The results of such calculations, based on a consecutive reaction as a model for oil shale pyrolysis, are much better than those for a single first-order model.

Table of symbols

A	— reactant symbol in the stoichiometric equation
A	— Arrhenius frequency factor, min^{-1}
DSC	— differential scanning calorimetry—rate of heat absorption, J/min
DTG	— rate of mass change, g/min
E	— Arrhenius activation energy, kJ/mol
f_1, f_2, f_3, f_4	— stoichiometric coefficient, Eqs (3a) and (3b)
G_1, G_2	— volatile products in the thermal degradation of kerogen
K_1, K_2, K_3	— kerogen and different solid products
k	— reaction rate constant, min^{-1}
m	— mass of corresponding compounds, g
q	— heating rate, deg/min
Q	— heat of reaction, J/mol
$\bar{Q}$	— ratio of reaction heats of the first and second stages in the consecutive reaction
r	— rate of reaction
R	— symbols for intermediate compounds in the consecutive reaction
R	— universal gas constant, 8.314 J/mol·K
S	— symbol of the final product in the consecutive reaction
T	— temperature, K
$T_m = T_2$	— temperature of DSC maximum (Eq. (1)), K
$T_m = T_1$	— temperature of DTG maximum, K

Index

A	— component A
R	— component R
S	— component S
1	— first stage of the consecutive reaction
2	— second stage of the consecutive reaction

* * *

The authors are greatful for financial support to the KFA International Bureau D–5170 Jülich on the German side, and to the Research Fund of the Belgrade Region Business Association for the Exploration, Production and Exploitation of Oil Shales, Belgrade, and SOUR Jugopetrol, Belgrade on the Yugoslavian side.

References

1 J. P. Elder, J. Thermal Anal., 29 (1984) 1327.
2 R. K. Agrawal, J. Thermal Anal., 31 (1986) 1253.
3 D. R. Dowdy, J. Thermal Anal., 32 (1987) 137.
4 D. R. Dowdy, J. Thermal Anal., 32 (1987) 1177.
5 D. Skala, H. Kopsch, M. Sokić, H.-J. Neumann and J. Jovanović, Fuel, 66 (1987) 1185.
6 V. M. Gorbachev, J. Thermal Anal., 8 (1975) 349.
7 ASTM E–698 standard.
8 H. E. Kissinger, J. Resp. Nat. Bur. Stds., 57 (1956) 217.
9 D. Skala, M. Sokić and H. Kopsch, Int. Congress on Thermal Analysis, Jerusalem, August 1988.
10 K. O. V. Engler, Die Chemie und Physik des Erdöls, Vol. 1, S. Hirzel, Leipzig, 1913.
11 R. L. Braun and A. J. Rothman, Fuel, 54 (1975) 129.
12 A. K. Burnham, ACS Symp. Ser., 163 (1981) 39.
13 F. P. Miknis, T. F. Turner, G. L. Berdan and P. J. Conn, Energy and Fuels, 1 (1987) 477.
14 J. H. Campbell, G. J. Koskinas, G. Gallegos and M. Gregg, Fuel, 59 (1980) 718.
15 B. Horsfield, "Pyrolysis Studies and Petroleum Exploration" in Advances in Petroleum Geochemistry, Vol. 1, p. 247–298, Eds J. Brooks and D. Welte, Academic Press, London 1984.

Zusammenfassung — Unter Annahme eines komplexen Mechanismus für thermische Abbauprozesse wurde für den Reaktionstyp $A \xrightarrow{k_1} R \xrightarrow{k_2} S\uparrow$ eine theoretische analyse von DTG- und DSC-Kurven, gefolgt von einer entsprechenden mathematischen Simulation durchgeführt. Hier stellt die Verbindung S ein flüchtiges Produkt dar (Gas oder Dampf), was eine notwendige Bedingung zur Erklärung von unterschiedlichen Ergebnissen nach der kinetischen Analyse der experimentellen DTG- und DSC-Daten ist. Bei der mathematischen Simulation wurden unterschiedliche Arrheniusparameterwerte benutzt, für beide Reaktionsgeschwindigkeitskonstanten (k_1 und k_2) in einem Intervall von 83,1–291,0 kJ/mol für die Aktivierungsenergie sowie unter Anwendung entsprechender Frequenzfaktoren (10^5–10^{19} min^{-1}). Für die Reaktionen $A \rightarrow R$ und $R \rightarrow S$ wurde auch der Einfluß von endothermen Wärmeeffekten (50–200 kJ/mol) untersucht. Die berechneten Geschwindigkeiten für die Veränderung von Masse und Wärme (DTG und DSC) bei verschiedenen Aufheizgeschwindigkeiten zeigen, daß beide Kurven ihr Maximum bei unterschiedlichen Temperaturen erreichen. Die Ungleichmäßigkeit der DTG- und DSC-Maxima basiert auf den unterschiedlichen Werten der Reaktionsgeschwindigkeitskonstanten, deren Temperaturempfindlichkeit (E_1 und E_2) und hängt auch von der Aufheizgeschwindigkeit ab. Die durchgeführte theoretische Analyse zeigt, daß es mit Hilfe simultaner DTG- und DSC-Untersuchungen möglich ist, im Falle konsekutiver Reaktionen erster Ordnung die Reaktionsgeschwindigkeitsparameter (k_1 und k_2) zu bestimmen. Das vorgeschlagene theoretische Analysenverfahren wird am Beispiel der experimentellen DTG/DSC-Daten der Pyrolyse von Ölschiefer und Anwendung konsekutiver Reaktionen illustriert.

Резюме — Для реакции типа $A \xrightarrow{\kappa_1} R \xrightarrow{\kappa_2} S\uparrow$ предложен сложный механизм процессов термического распада и с помощью математического моделирования проведен теоретический анализ кривых ДТГ и ДСК. В такой схеме реакции соединение S представляет летучий продукт (напр. газ или пар), что является необходимым предположением для объяснения различия результатов, возникших после кинетического анализа экспериментальных данных ДТГ и ДСК. Математическое моделирование проводилось используя различные значения аррениусовского параметра для обоих реакционных констант скорости (κ_1 и κ_2) в области значений энергий активации 83,1–291,0 кдж·моль$^{-1}$ и с соответствующими значениями частотного множителя (10^5–10^{19} мин$^{-1}$). Изучено также влияние эндотермических тепловых эффектов (50–200 кдж·моль$^{-1}$) для реакций $A \rightarrow R$ и $R \rightarrow S$. Вычисленные скорости потери веса и тепла (ДТГ и ДСК) при различных скоростях нагрева показали, что максимальные значения обоих кривых достигаются при различных температурах. Несовпадение максимумов ДТГ и ДСК зависит от различия между значениями реакционных констант скоростей и их температурной чувствительностью (E_1 и E_2), также ка и от скорости нагрева. Проведенный теоретический анализ показал, что при использовании совмещенного ТГ и ДСК анализа представляется возможность определения реакционных параметров κ_1 и κ_2 в случае последовательных реакций первого порядка. Предложенный теоретический анализ подтвержден экспериментальными ДТГ/ДСК данными пиролиза сланцевого дегтя, которые были интерпретированы на основе последовательных реакций.